



Circumpolar transport of a volcanic cloud from Hekla (Iceland)

S. A. Carn,¹ A. J. Prata,² and S. Karlsdóttir³

Received 28 January 2008; revised 26 March 2008; accepted 31 March 2008; published 31 July 2008.

[1] Hekla volcano (Iceland) erupted on 17 August 1980 and emplaced a sulfur dioxide (SO₂) cloud into the north polar stratosphere at a maximum altitude of ~15 km. The SO₂ is tracked using satellite data from the ultraviolet (UV) Nimbus-7 Total Ozone Mapping Spectrometer (N7/TOMS) and the infrared (IR) High-resolution Infrared Radiation Sounder (HIRS/2) on the NOAA TIROS Operational Vertical Sounder (TOVS) platform. The eruption emitted ~0.5–0.7 Tg of SO₂, which later split into three distinct clouds, one of which circled the North Pole at the perimeter of an atypically persistent Arctic cyclone for six days, impacting airspace on three continents. Separate clouds drifted across eastern Russia, Alaska, and Canada. Maximum SO₂ columns derived from TOMS and HIRS/2 accurately define the volcanic cloud's path and fit trajectories produced by the NOAA Hybrid Single-Particle Lagrangian Integrated Trajectory (HYSPLIT) model, providing confidence in the model. When combined with the SO₂ measurements, trajectory altitudes derived from HYSPLIT provide robust estimates of the altitudes of the SO₂ clouds (8–15 km), which would be elusive using either the satellite data or the trajectory model in isolation. Near-coincident, spectrally discrete UV and IR retrievals are compared in the volcanic cloud and indicate good agreement between TOMS and HIRS/2 SO₂ columns for pixels with similar viewing geometry. Hekla eruptions, which follow a pattern of early explosive venting of volcanic gases with significant stratospheric injection, could play a role in promoting Arctic ozone loss, depending on the phase of the North Atlantic Oscillation during the eruption.

Citation: Carn, S. A., A. J. Prata, and S. Karlsdóttir (2008), Circumpolar transport of a volcanic cloud from Hekla (Iceland), *J. Geophys. Res.*, 113, D14311, doi:10.1029/2008JD009878.

1. Introduction

[2] Sulfur dioxide (SO₂) is an excellent tracer of atmospheric motions, particularly when injected into the upper troposphere/lower stratosphere (UTLS) by explosive volcanic eruptions. Eruptions release SO₂ from a well-defined source, typically at a well-constrained time, into an atmosphere normally free of background SO₂. It has a relatively long residence time (days to months) in the UTLS, permitting multiple consecutive observations, and can be easily measured using strong absorption features at ultraviolet (UV) or infrared (IR) wavelengths. In this paper we present a unique set of measurements following an explosive eruption of Hekla volcano (Iceland) in August 1980, which illuminates the dynamics of the summertime Arctic stratosphere.

[3] Monitoring of volcanic SO₂ emissions is a critical component of climate research since SO₂ is a precursor of sulfate aerosol, an agent of negative climate forcing (cooling) whose direct and indirect effects are a poorly constrained aspect of climate models [IPCC, 2001]. Volcanic

degassing provides a significant and persistent flux of SO₂ to the atmosphere [e.g., Graf *et al.*, 1997], and large explosive eruptions can inject a substantial part of their total SO₂ output into the stratosphere with accordingly longer gas and aerosol residence times. Current knowledge of volcanic SO₂ emissions in the UTLS is based primarily on measurements made by the four polar-orbiting, UV Total Ozone Mapping Spectrometer (TOMS) instruments successfully deployed between 1978 and 2005 [Bluth *et al.*, 1993; Krueger *et al.*, 2000; Carn *et al.*, 2003] and by the Ozone Monitoring Instrument (OMI) since 2004 [Yang *et al.*, 2007; Carn *et al.*, 2007].

[4] Techniques that exploit the strong absorption of IR radiation at ~7.34 μm by SO₂ have recently emerged [Prata *et al.*, 2003], which are capable of providing a complementary SO₂ climatology. Several satellite sensors possess a channel covering the 7.3 μm region (e.g., the Moderate Resolution Imaging Spectroradiometer [MODIS] and the Atmospheric Infrared Sounder [AIRS]) [Watson *et al.*, 2004; Carn *et al.*, 2005; Prata and Bernardo, 2007], but the one offering the longest data span is the High-resolution Infrared Radiation Sounder (HIRS/2) in NOAA's TIROS Operational Vertical Sounder (TOVS) package [Smith *et al.*, 1979]. HIRS/2 was first launched on the TIROS-N satellite in 1978 and has provided uninterrupted coverage from NOAA's polar-orbiting meteorological satellites since then. Since 1994 there have been 4 HIRS/2 instruments (or the

¹Joint Center for Earth Systems Technology (NASA/UMBC), University of Maryland Baltimore County, Baltimore, Maryland, USA.

²Atmosphere and Climate Department, Norwegian Institute for Air Research (NILU), Kjeller, Norway.

³Icelandic Meteorological Office, Reykjavik, Iceland.

Table 1. Specifications of the TOMS and HIRS/2 Instruments Operational in 1980

	TOMS	HIRS/2
Spacecraft	Nimbus-7	TIROS-N, NOAA-6
Orbit inclination	99.1°	98.9°, 98.7°
Orbital period, min	104.15	102.1, 101
Ascending node (local time)	12:00	15:00, 19:30
Spectral range, μm	0.31–0.38	0.7–15
Field of view (FOV), mrad	52.4	21.8
Ground FOV: nadir	50 km square	17.7 km circular
Ground FOV: scan edge, km	125 \times 280	31.8 \times 62.8
Scan line		
Scan time, s	8	6.4
Scan angle	$\pm 51^\circ$	$\pm 49.5^\circ$
Swath width, km	3000	2240
Pixels per scan line	35	56
Distance between pixels		
Cross-track	variable	26.4 km
Along track	variable	41.8 km

more recent iterations, HIRS/3 and HIRS/4) in orbit simultaneously [Prata *et al.*, 2003].

[5] TOMS measured the albedo of the sunlit Earth's atmosphere at six wavelengths between 0.31 and 0.38 μm and permitted daily, low spatial resolution observations of volcanic clouds at most latitudes (Table 1). The TOMS SO₂ algorithm [Krueger *et al.*, 1995, 2000] employs a linear model of Rayleigh scattering and absorption by SO₂ and ozone that is solved simultaneously at four TOMS wavelengths. TOMS is most sensitive to SO₂ in the UTLS since most UV radiation is scattered or reflected back to space before reaching the Earth's lower atmosphere and surface. IR measurements use emitted radiation and hence complement the UV techniques by permitting both daytime and nocturnal retrievals of SO₂ in volcanic clouds, therefore increasing the frequency of observations during cloud dispersal and transport. The SO₂ absorption feature centered at $\sim 7.3 \mu\text{m}$ that is covered by HIRS/2 is located in a spectral region with significant absorption by water vapor, which limits HIRS/2 retrievals to SO₂ located above the peak in the water vapor weighting function, which is typically at $\sim 3 \text{ km}$ [Prata *et al.*, 2003]. TOMS and HIRS/2 are therefore somewhat similar in their increased sensitivity to SO₂ in the UTLS. Both sensors are also able to detect volcanic ash (see section 3).

[6] Validation is needed to ratify long-term records such as the TOMS volcanic SO₂ data base [Bluth *et al.*, 1993; Carn *et al.*, 2003], but opportunities were infrequent, and SO₂ validation in general is challenging. Noneruptive volcanic plumes that have been monitored regularly using ground-based or airborne instruments (e.g., correlation spectrometer [COSPEC]) were usually not sufficiently large or concentrated for detection by TOMS, and comparisons of TOMS and ground-based data have only been possible at two major SO₂ emitters; Popocatepetl (Mexico) [Schaefer *et al.*, 1997] and Nyiragongo (D.R. Congo) [S. A. Carn, unpublished data]. Otherwise, validation of TOMS SO₂ retrievals relied on the serendipitous transit of a volcanic cloud over a Brewer spectrophotometer station or other ground-based instrument, which occurred only three times during the TOMS missions [Krueger *et al.*, 2000]. Development of IR SO₂ retrieval techniques offers many new

opportunities for satellite-based validation of UV SO₂ measurements, and the 1980 Hekla eruption studied here permits a comparison between UV Nimbus-7 (N7) TOMS and IR HIRS/2 retrievals of SO₂ in a relatively long-lived stratospheric volcanic cloud.

[7] The 1980 Hekla eruption is unique in the 30-year history of TOMS and OMI volcanic SO₂ measurements, being the only event known to have produced a cloud that circumnavigated the North Pole at high latitudes (Figure 1). As such it is of value as a tracer of polar stratospheric dynamics, similar to the Cerro Hudson eruption of August 1991, which produced a long-lived stratospheric SO₂ cloud that encircled Antarctica [Barton *et al.*, 1992; Schoeberl *et al.*, 1993]. Orbits of polar-orbiting satellites converge toward the poles and the high latitudes (60–80°N) reached by the 1980 Hekla emissions, combined with the timing of the eruption in the northern hemisphere summer (when the UV terminator is at high latitudes), allowed for an unprecedented frequency of observations by TOMS and HIRS/2. Since TOMS SO₂ measurements have been validated to some extent using ground-based data [Schaefer *et al.*, 1997; Krueger *et al.*, 2000] they provide a useful reference for other methods. Independent HIRS/2 retrievals permit further assessment of the UV measurements, whilst agreement between the two methods corroborates the IR data as a reliable alternative. Integrating the two data sets, thereby increasing the frequency of cloud observations, also elucidates the dispersal of volcanic clouds after eruption.

[8] Here we demonstrate that integrated satellite SO₂ measurements may be used to test air parcel trajectory models. Such models are used to predict volcanic cloud trajectories for aviation hazard mitigation. Encounters with volcanic ejecta can be a significant hazard to aircraft, even at great distances from the source volcano [e.g., Casadevall, 1994]. Although ash is the salient hazard to aviation, transit through ash-poor clouds can also result in costly damage to aircraft components [e.g., after the 2000 Hekla eruption; Grindle and Burcham, 2002; Rose *et al.*, 2003] and gases such as SO₂, and derived acid aerosol, usually have a longer lifetime than coemitted ash. Moreover, in many explosive eruptions observed using satellite data, ash-rich and SO₂-rich portions of the discharged cloud have separated and followed different trajectories at distinct altitudes as a result of wind shear [e.g., Schneider *et al.*, 1999; Constantine *et al.*, 2000; Carn *et al.*, 2002]. Long-range posteruption trajectory forecasts are hence expedient, and evaluation of trajectory models is needed, but as Tupper *et al.* [2004] have noted, the detection period for a drifting ash cloud is typically only 2–12 hours posteruption using a single IR or VIS channel. In a dry atmosphere with no significant meteorological clouds Tupper *et al.* [2004] were able to track an ash cloud for ~ 80 hours using geostationary IR split-window imagery, but such conditions are unusual. We show that long-lived SO₂ clouds in the UTLS are conducive to trajectory model evaluation, and use the 1980 Hekla case to demonstrate that combining multitemporal satellite observations of SO₂ with such models can refine cloud altitude estimates.

2. The 1980 Hekla Eruption

[9] Hekla (63.98°N, 19.7°W, alt. 1491 m) is one of Iceland's most active volcanoes and is responsible for some

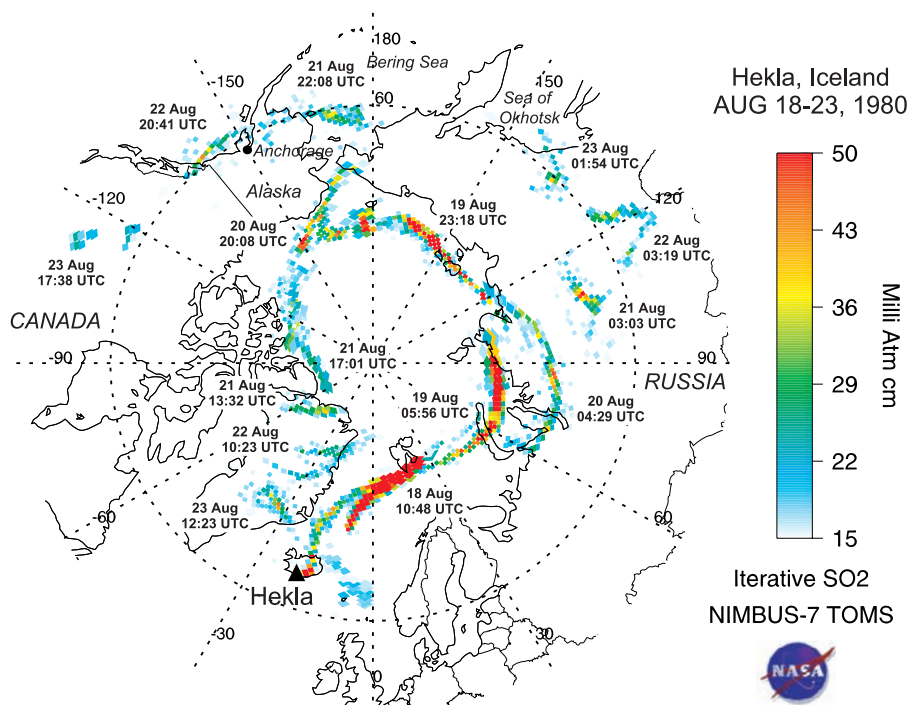


Figure 1. Composite map of N7/TOMS SO₂ retrievals for the 1980 Hekla eruption cloud. Dates and times of each cloud observation are indicated. For clarity, some of the orbits listed in Tables 2, 3, and 4 have been omitted. The color scale is cut off at 15 DU, which is the approximate SO₂ detection limit (3σ noise level) for N7/TOMS.

of the country's largest historical eruptions. Its 17 August 1980 eruption was the second in a roughly decennial series that began in 1970 and continued in 1991 and 2000 [Thorarinsson and Sigvaldason, 1972; Grönvold *et al.*, 1983; Gudmundsson *et al.*, 1992; Höskuldsson *et al.*, 2007], signaling an increased eruption rate after a major plinian event in 1947 [Thorarinsson, 1967]. At the time, the 1980 eruption was distinguished by the very short repose time preceding the event (10 years following the 1970 eruption), which was the shortest on record since Hekla's first historical eruption in 1104 [Grönvold *et al.*, 1983], although subsequent eruptions have also been separated by only 9–10 years. Each of the three Hekla eruptions since 1980 produced SO₂ clouds that were detected by a TOMS instrument [Carn *et al.*, 2003; <http://toms.umbc.edu>] and also by HIRS/2 [Prata *et al.*, 2003; Rose *et al.*, 2003]. Eruptions from Icelandic volcanoes potentially threaten the busy North Atlantic air corridor, but the 1980 and 1991 Hekla eruptions both produced long-lived SO₂ clouds that traveled a large distance from Iceland (reaching central Asia in the latter case) and hence impacted airspace far from the source region [e.g., Prata *et al.*, 2003].

[10] The 1980 eruption began abruptly at 13:27 LT (local time, equivalent to UTC in Iceland) on 17 August when a dark plinian column emerged from Hekla, which was rapidly overtaken by a steam column that reached a maximum reported height of 15 km by 14:00 LT [SEAN, 1980; Grönvold *et al.*, 1983]. Tephra was carried northward and ash fall continued for up to 6 hours in distal locations (up to 200 km NNE of Hekla), consistent with radar measurements that showed a significant decline in cloud size between

18:00 and 19:00 LT [Grönvold *et al.*, 1983]. Effusion of lava flows from the eruptive fissure began only 3 minutes after initiation of the plinian phase, and continued until the end of significant eruptive activity on 20 August, although the lava production rate had declined notably by 18 August. The eruption produced a total of 120 million m³ of lava and 60 million m³ of tephra [Grönvold *et al.*, 1983]. A much smaller eruption of Hekla in April 1981 is considered a continuation of the August 1980 event [Grönvold *et al.*, 1983]. N7/TOMS also detected very weak SO₂ emissions associated with the April 1981 eruption but these are not considered in this paper.

[11] Photographs and observations of Hekla eruptions [e.g., Thorarinsson, 1967; Grönvold *et al.*, 1983; Höskuldsson *et al.*, 2007] and recent satellite-based investigations [e.g., Rose *et al.*, 2003] indicate that the volcanic clouds produced by Hekla since 1947 have been characteristically gas rich and ash poor, perhaps due to early venting of accumulated gases combined with rapid fallout of tephra. In this respect the 1980 eruption was typical; very little airborne ash was detected by both TOMS and HIRS/2, although it is likely that the presence of fine ash, which was suggested by in situ aircraft measurements in the February 2000 eruption cloud [Pieri *et al.*, 2002; Hunton *et al.*, 2005], was masked by the formation of ice in the plume at an early stage [e.g., Rose *et al.*, 1995, 2003]. Another salient and somewhat unusual attribute of Hekla's eruption clouds since 1970 has been an early abundance of fine sulfate aerosol and sulfuric acid [Cadle and Blifford, 1971; Rose *et al.*, 2003], which in 2000 was apparent as early as ~ 3 hours after the eruption and at peak mass amounted to 2–5% of the SO₂ mass in the same cloud

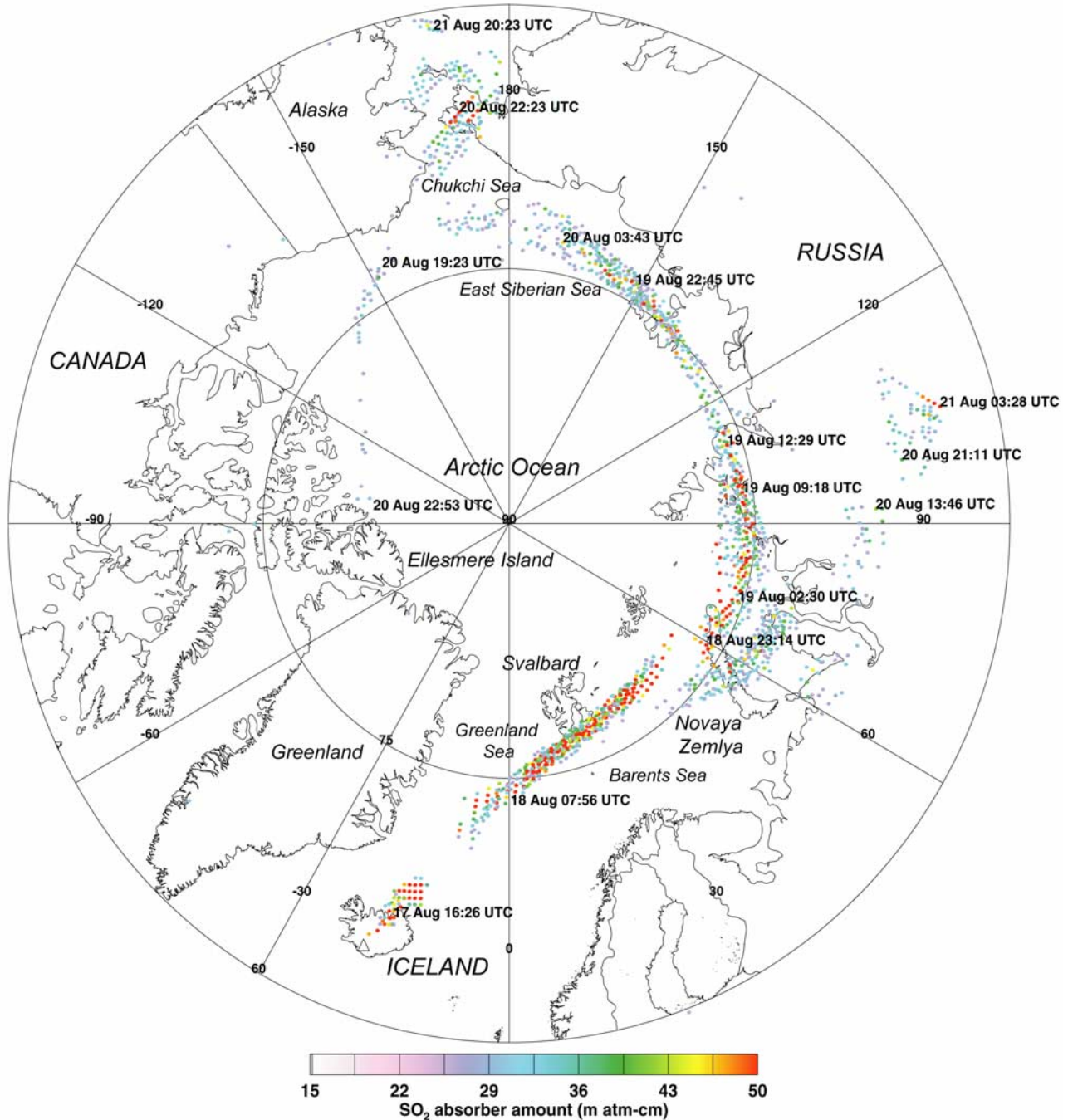


Figure 2. Composite map of HIRS/2 SO₂ retrievals for the 1980 Hekla eruption cloud. Dates and times of each cloud observation are indicated. For clarity, only a subset of the orbits listed in Tables 2–4 is shown.

[Rose *et al.*, 2003]. The precise origin of this sulfate is not well understood.

3. Satellite and Model Data

[12] During the 1980 Hekla eruption N7/TOMS was operational and the HIRS/2 sensor was in orbit on the TIROS-N and NOAA-6 satellites (hereafter termed TN HIRS and N6 HIRS respectively). Specifications of these instruments are given in Table 1. Figures 1 and 2 do not

show the full set of SO₂ retrievals available from TOMS and HIRS/2; in both cases the complete data set may be obtained on request from the lead authors.

3.1. Nimbus-7 TOMS

[13] The Hekla SO₂ clouds were tracked using the version 7 TOMS production SO₂ algorithm, termed the sulfur dioxide index (SOI) [McPeters *et al.*, 1996], and an offline SO₂ retrieval described by Krueger *et al.* [1995, 2000]. The SOI is essentially a flag denoting inconsistencies in ozone

retrievals using different TOMS wavelengths, and is useful for mapping the locations of SO₂ clouds, while the offline algorithm is used for quantitative SO₂ measurements. N7/TOMS could also simultaneously detect UV absorbing aerosol (e.g., volcanic ash, dust) and nonabsorbing aerosol (e.g., sulfate) using the spectral contrast between calculated and observed radiances at 340 and 380 nm, termed the Aerosol Index (AI) [Seftor *et al.*, 1997]. The TOMS AI is positive for UV absorbing aerosols, negative for nonabsorbing particles and near zero for water/ice clouds (although large optical depths of ice [>3] can also produce a small negative AI signal) [e.g., Rose *et al.*, 2003].

[14] No information on the height of volcanic clouds can be directly retrieved from TOMS data, although the altitudinal range of a volcanic cloud can sometimes be inferred if opaque meteorological clouds of known altitude are present in the scene, and the SO₂ overlies these clouds. However, since the retrieved amount of SO₂ is altitude dependent (owing to the temperature dependence of the SO₂ absorption cross-section and variable radiative transfer), an altitude is assumed in the TOMS SO₂ retrieval algorithm. The default altitude for volcanic clouds in the UTLS is 20 km.

[15] Errors in TOMS SO₂ retrievals are highly specific to the particular measurement conditions, but in general they are lowest ($\pm 10\%$) for compact, aerosol-free clouds illuminated at low to moderate solar zenith angles (SZA) in the UTLS [Krueger *et al.*, 1995]. The 1980 Hekla clouds were mostly situated above 60°N with correspondingly high SZAs; under these conditions retrieval errors are larger ($\pm 30\%$) [Krueger *et al.*, 1995]. Moderate optical depths of volcanic ash and sulfate aerosol collocated with the SO₂ result in overestimates of 15–25%. Aerosol-induced biases are dependent on particle size and composition, which are rarely known for volcanic clouds in the UTLS, and this information is not available for the 1980 Hekla case. However, as discussed below the N7/TOMS AI data indicate that the emitted cloud was ash poor even in the first available TOMS overpass, so errors due to ash are assumed to be minimal. Sulfate aerosol also appeared much less abundant in the 1980 cloud than in the February 2000 emissions [Rose *et al.*, 2003] although the 2000 eruption was observed by Earth Probe (EP) TOMS using different AI wavelengths, which influences the AI signal. The reflectivity of the surface or clouds underlying the SO₂ also impacts UV retrievals, and SO₂ amounts measured in the 1980 Hekla cloud were probably affected during transit of the cloud over sea ice and the Greenland ice cap (see later discussion). Finally, calculation of SO₂ mass in volcanic clouds requires a correction for background biases, which is most easily accomplished for compact, concentrated clouds. The 1980 Hekla clouds were nonideal in this respect, being highly elongate in form throughout the period of atmospheric residence (Figure 1), and few individual orbits contained the entire cloud (Tables 2, 3, and 4).

[16] Despite its modest size, the 1980 Hekla eruption cloud is highly conducive to multispectral studies using polar-orbiting satellites due to its occurrence at high latitudes in the northern hemisphere summer. For a period around the summer solstice for each pole, TOMS is able to measure backscattered sunlight from the regions on the descending (north to south) part of the orbit lit by the midnight sun. This configuration produced 4–7 TOMS

orbits per day containing the SO₂ cloud and increased the likelihood of coincidence between TOMS and HIRS/2. The ash-poor nature of the eruption minimized any interference due to volcanic ash (which affects UV retrievals) [Krueger *et al.*, 1995], even in the initial stages of cloud transport. The relatively long atmospheric residence time of the SO₂ allowed for retrievals under a variety of viewing and background conditions and the dry polar atmosphere also reduced the impact of water vapor on IR retrievals (see below).

3.2. NOAA HIRS/2

[17] SO₂ retrieval using HIRS/2 data utilizes the strong asymmetric stretch absorption of the gas at 7.34 μm , which is close to the central wavelength of HIRS/2 channel 11 [7.33 μm ; Prata *et al.*, 2003]. Prata *et al.* [2003] provide a detailed description of the retrieval technique, summarized here, which uses an accurate transmittance model to relate absorption in HIRS/2 channel 11 to SO₂ absorber amount. Using the model, a look-up table (LUT) relating observed transmittance to SO₂ column amount is computed for 26 atmospheric layers at varying temperature and pressure, and the HIRS/2 channel 11 filter functions for each satellite. To derive SO₂ layer transmittance from HIRS/2 temperature measurements, the algorithm assumes that an isothermal layer of SO₂ is embedded in an otherwise clear atmosphere, with the SO₂ located above the peak of the weighting function for H₂O in the 7.3 μm channel. As for TOMS, SO₂ layer altitude cannot be retrieved directly from HIRS/2 data, so an independent estimate of the SO₂ cloud altitude is required to generate the appropriate absorber amount LUT (the dependence on pressure is stronger than that on temperature). In this case an altitude of 11 km was assumed for all HIRS/2 retrievals.

[18] The technique relies on an estimate of the background radiance (unperturbed by SO₂), which is obtained by interpolation of radiances in adjacent HIRS/2 channels. This can be inaccurate for mixed pixels containing clear sky and clouds [Prata *et al.*, 2003]. Because the 7.3 μm channel is sensitive to water vapor, SO₂ lying below significant water vapor will be undetectable by HIRS/2, which limits the retrieval to SO₂ above 3 km altitude in clear conditions [Prata *et al.*, 2003]. Water/ice clouds located above the SO₂ have a similar masking effect. Residual water vapor absorption can cause anomalies in the retrieval, particularly if large amounts of water vapor are located just below a thin SO₂ layer, or if unusual atmospheric conditions result in atypical vertical water vapor distributions. Tests are employed to remove obvious water vapor anomalies. Thermal contrast is also a limiting factor, and can inhibit retrievals for any situation in which the SO₂ cloud is at a similar temperature to the underlying surface, for example when optically thin SO₂ clouds overlie very cold surfaces such as ice- or snow-covered ground [Prata *et al.*, 2003]. Prata *et al.* [2003] report lower detection limits of ~ 5 DU for SO₂ clouds at 5 km altitude, and ~ 20 DU for clouds at 35 km altitude, with typical errors of 5–10%.

[19] For our study of the 1980 Hekla eruption, a total of 41 NOAA-6 orbits and 16 TIROS-N orbits were used for HIRS/2 SO₂ retrievals. Observations were impeded when the TOVS calibration sequence, when no Earth data are

Table 2. Selected UV and IR Retrievals of SO₂ in the 1980 Hekla Volcanic Cloud that Circled the N. Pole

Date	Time (UT)	Sensor	SO ₂ Mass (Tg)	SO ₂ Max (DU) ^a	Lat ^b	Lon ^b	Scan Position ^c	
17 Aug	1627	TN HIRS	0.002	40	66	-16.93	50	
	1817	N6 HIRS	0.012	48	65.9	-17.34	7	
	1958	N6 HIRS	0.036 ^d	108	68.22	-14.2	46	
18 Aug	0723	TOMS	0.489 ^d	107	74.56	3.78	27	
	0757	N6 HIRS	0.119 ^d	119	74.52	3.31	50	
	0906	TOMS	0.420 ^d	159	75.54	6.69	16	
	0933	TN HIRS	0.066 ^d	93	75.33	5.72	9	
	1048	TOMS	0.470	142	76.1	13.04	4	
	1116	N6 HIRS	0.094 ^d	124	77.04	22.64	13	
	1231	TOMS	0.173 ^d	75	64.73	-15.96	7	
	1255	N6 HIRS	0.088 ^d	118	76.93	25.35	13	
	1434	N6 HIRS	0.084 ^d	104	77.48	34.57	30	
	1615	N6 HIRS	0.098 ^d	90	77.44	40.21	n/a	
	2314	TN HIRS	0.059 ^d	108	76.01	59.25	56	
	19 Aug	0049	N6 HIRS	0.063 ^d	68	76.69	100.09	55
0056		TN HIRS	0.041 ^d	101	75.86	69.3	36	
0230		TOMS	0.193 ^d	129	75.59	74.26	26	
0231		N6 HIRS	0.044 ^d	75	75.3	71.81	56	
0412		TOMS	0.129 ^d	188	75.4	78.15	17	
0551		N6 HIRS	0.058 ^d	114	75.34	83.63	14	
0556		TOMS	0.433	136	75.75	86	4	
0730		N6 HIRS	0.061 ^d	80	75.55	89.49	8	
0740		TOMS	0.146 ^d	60	75.57	74.4	1	
0910		N6 HIRS	0.144 ^d	99	75.7	95	13	
0918		TN HIRS	0.036 ^d	66	75.63	94.5	54	
1049		N6 HIRS	0.069 ^d	81	75.68	101.81	34	
1230		N6 HIRS	0.050 ^d	72	75.94	109.17	55	
1757		TN HIRS	0.010 ^d	30	74.62	138.92	56	
1938		TN HIRS	0.025 ^d	66	74.94	139.42	42	
2105		N6 HIRS	0.010 ^d	28	73.51	175.98	42	
2119		TN HIRS	0.024 ^d	62	74.87	142.14	19	
2246		N6 HIRS	0.046 ^d	49	73.98	151.28	42	
2259		TN HIRS	0.026 ^d	57	73.94	152.33	6	
2318		TOMS	0.164 ^d	108	74.21	153.05	18	
20 Aug	0026	N6 HIRS	0.046 ^d	55	74.29	154.37	17	
	0039	TN HIRS	0.028 ^d	52	74.16	157.26	9	
	0102	TOMS	0.257 ^d	92	73.71	160.75	4	
	0205	N6 HIRS	0.057 ^d	49	73.84	160.95	5	
	0344	N6 HIRS	0.052 ^d	53	73.16	168.76	5	
	0523	N6 HIRS	0.039 ^d	32	73.36	175.42	21	
	0703	N6 HIRS	0.024 ^d	33	73.77	172.81	44	
	0845	N6 HIRS	0.017 ^d	32	74.66	156.84	51	
	1536	N6 HIRS	0.011 ^d	26	80.16	-126.24	n/a	
	1642	TOMS	0.106 ^d	47	79.45	-124.6	16	
	1718	N6 HIRS	0.031 ^d	32	79.54	-123.17	n/a	
	1825	TOMS	0.273 ^d	57	73.58	-151.6	26	
	1923	TN HIRS	0.005 ^d	30	73.51	-151.23	5	
	2008	TOMS	0.442	56	73.33	-151.59	15	
	2151	TOMS	0.168 ^d	53	74.78	-159.06	6	
	2359	N6 HIRS	0.006 ^d	32	74.83	-143.68	7	
	21 Aug	1332	TOMS	0.061 ^d	39	82.05	-44.16	6
		1653	N6 HIRS	0.003 ^d	11	80.91	-41.52	27
		1701	TOMS	0.263 ^d	28	83.12	-92.5	5
	22 Aug	1736	TN HIRS	0.014 ^d	58	61.09	-171.51	2
0839		TOMS	0.018 ^d	33	78.61	-21.16	21	
1023		TOMS	0.040 ^d	31	77.76	-29.93	19	
23 Aug	1206	TOMS	0.122	42	77.42	-27.98	10	
	1040	TOMS	0.038 ^d	31	63.79	-4.18	21	
	1223	TOMS	0.117	45	70.12	-33.32	17	

^aMaximum retrieved SO₂ column amount in each orbit.^bCenter location of pixel containing maximum SO₂ column.^cRanges from 1–35 for TOMS, 1–56 for HIRS/2. The smallest FOV (nadir) occurs at the midpoint of the scan.^dDenotes orbits with partial coverage of the SO₂ cloud.

collected for the equivalent of 3 scan lines, intersected the SO₂ cloud.

3.3. HYSPLIT Model

[20] The HYbrid Single-Particle Lagrangian Integrated Trajectory (HYSPLIT₄) model [Draxler and Rolph,

2003; Rolph, 2003] was used to calculate both forward and backward trajectories of discrete air parcels for comparison with satellite-derived volcanic cloud trajectories. CDC1 global reanalysis meteorological data were used for the HYSPLIT runs. The combined TOMS and HIRS/2 SO₂ observations were used to define the observed trajectory and

Table 3. Selected UV and IR SO₂ Retrievals for the 1980 Hekla Volcanic Cloud that Drifted over Russia

Date	Time (UT)	Sensor	SO ₂ Mass (Tg)	SO ₂ Max (DU) ^a	Lat ^b	Lon ^b	Scan Position ^c
19 Aug	1410	N6 HIRS	0.026 ^d	42	72.12	73.84	49
20 Aug	0007	N6 HIRS	0.018 ^d	23	66.2	108.48	56
	0429	TOMS	0.240	48	69.05	86.61	17
	0613	TOMS	0.289	47	68.09	70.23	11
	1026	N6 HIRS	0.020 ^d	33	68.36	89.14	4
	1208	N6 HIRS	0.015 ^d	27	69.25	60.8	4
	1347	N6 HIRS	0.024 ^d	38	67.79	92.2	56
	2112	TN HIRS	0.012 ^d	35	65.98	98.92	51
	2253	TN HIRS	0.014 ^d	33	66.29	104.45	12
21 Aug	0149	N6 HIRS	0.022 ^d	34	64.23	104.21	31
	0303	TOMS	0.044 ^d	54	64.78	108.39	21
	0329	N6 HIRS	0.036 ^d	53	63.2	104.67	1
	0446	TOMS	0.071	42	64.15	108.98	3
	0632	TOMS	0.022 ^d	28	69.81	56.25	16
	1002	N6 HIRS	0.021 ^d	67	62.59	111.89	7
	1141	N6 HIRS	0.016 ^d	33	62.09	113.42	47
22 Aug	0136	TOMS	0.032 ^d	29	59.72	123.04	30
	0319	TOMS	0.042	35	57.99	121.74	9
23 Aug	0154	TOMS	0.012	39	60.76	136.24	14

^aMaximum retrieved SO₂ column amount in each orbit.

^bCenter location of pixel containing maximum SO₂ column.

^cRanges from 1–35 for TOMS, 1–56 for HIRS/2. The smallest FOV (nadir) occurs at the mid-point of the scan.

^dDenotes orbits with partial coverage of the SO₂ cloud.

dispersion of the volcanic clouds, and the cloud altitude in HYSPLIT model runs was iterated until the best fit between observed and model trajectories was obtained. No quantitative measure of the goodness of fit between the model and observations was used. Forward trajectories initialized at 1300 UT on August 17 (the closest HYSPLIT time step to the start of the eruption at 1327 UT) were used to constrain the cloud altitude, and then if observed and model endpoints did not coincide back trajectories were employed to check whether volcanic cloud positions were consistent with an origin from Hekla. Back trajectories were initialized at the time of the final satellite observation of the SO₂ cloud (in all cases derived from TOMS data). The height chosen in the model calculations was found to have a significant impact on the calculated trajectory (Figure 3).

4. Trajectory of the 1980 Hekla Volcanic Cloud

4.1. Satellite Observations

[21] N7/TOMS first detected the leading edge of the 1980 eruption cloud at 0541 UT on August 18, when it was just

crossing 0° longitude. The 1048 UT overpass was the first TOMS orbit containing the entire volcanic cloud at optimum scan positions (Table 2), and by that time the leading edge of the cloud had reached the Barents Sea at ~30°E, with a narrow arc of SO₂ extending back across the Greenland Sea and connected to Hekla (Figure 1). At 1048 UT the highest SO₂ column amounts were measured by TOMS in a compact region southwest of Svalbard (Figures 1 and 2), and the total SO₂ burden was ~0.5 Tg. The next TOMS overpass at 1231 UT on August 18 was the last time SO₂ was observed attached to Hekla, indicating a minimum venting period of ~23 hours. The next near-nadir TOMS overpass of Hekla occurred at 1106 UT on August 19 and no SO₂ emissions were apparent, although cloud cover could have obscured a low-level plume. The total SO₂ burden measured by TOMS never exceeded ~0.5 Tg in a single orbit (Table 2); it is conceivable that the total burden was larger but the precise SO₂ mass became difficult to establish as thereafter the cloud straddled several consecutive orbits.

Table 4. Selected UV and IR SO₂ Retrievals for the 1980 Hekla Volcanic Cloud that Drifted over Alaska and Canada

Date	Time (UT)	Sensor	SO ₂ mass (Tg)	SO ₂ max (DU) ^a	Lat ^b	Lon ^b	Scan Position ^c
20 Aug	1746	TN HIRS	0.010 ^d	28	68.02	-173.06	10
	1903	N6 HIRS	0.041 ^d	54	67.37	-175.53	56
	2008	TOMS	0.442	56	73.33	-151.59	15
	2044	N6 HIRS	0.040 ^d	54	66.33	-172.14	22
	2224	N6 HIRS	0.076 ^d	86	65.83	-172.86	1
21 Aug	0024	TN HIRS	0.044 ^d	79	64.87	-174.23	4
	0458	N6 HIRS	0.032 ^d	42	63.2	-178.81	3
	0638	N6 HIRS	0.049 ^d	35	63.36	-173.53	44
	1736	TN HIRS	0.012 ^d	58	61.09	-171.51	2
	2208	TOMS	0.071	38	60.75	-170.96	18
22 Aug	2041	TOMS	0.041	44	59.2	-140.38	10
	2226	TOMS	0.019 ^d	29	60.32	-166.98	10
23 Aug	1738	TOMS	0.031	26	53.83	-111.63	31

^aMaximum retrieved SO₂ column amount in each orbit.

^bCenter location of pixel containing maximum SO₂ column.

^cRanges from 1–35 for TOMS, 1–56 for HIRS/2. The smallest FOV (nadir) occurs at the mid-point of the scan.

^dDenotes orbits with partial coverage of the SO₂ cloud.

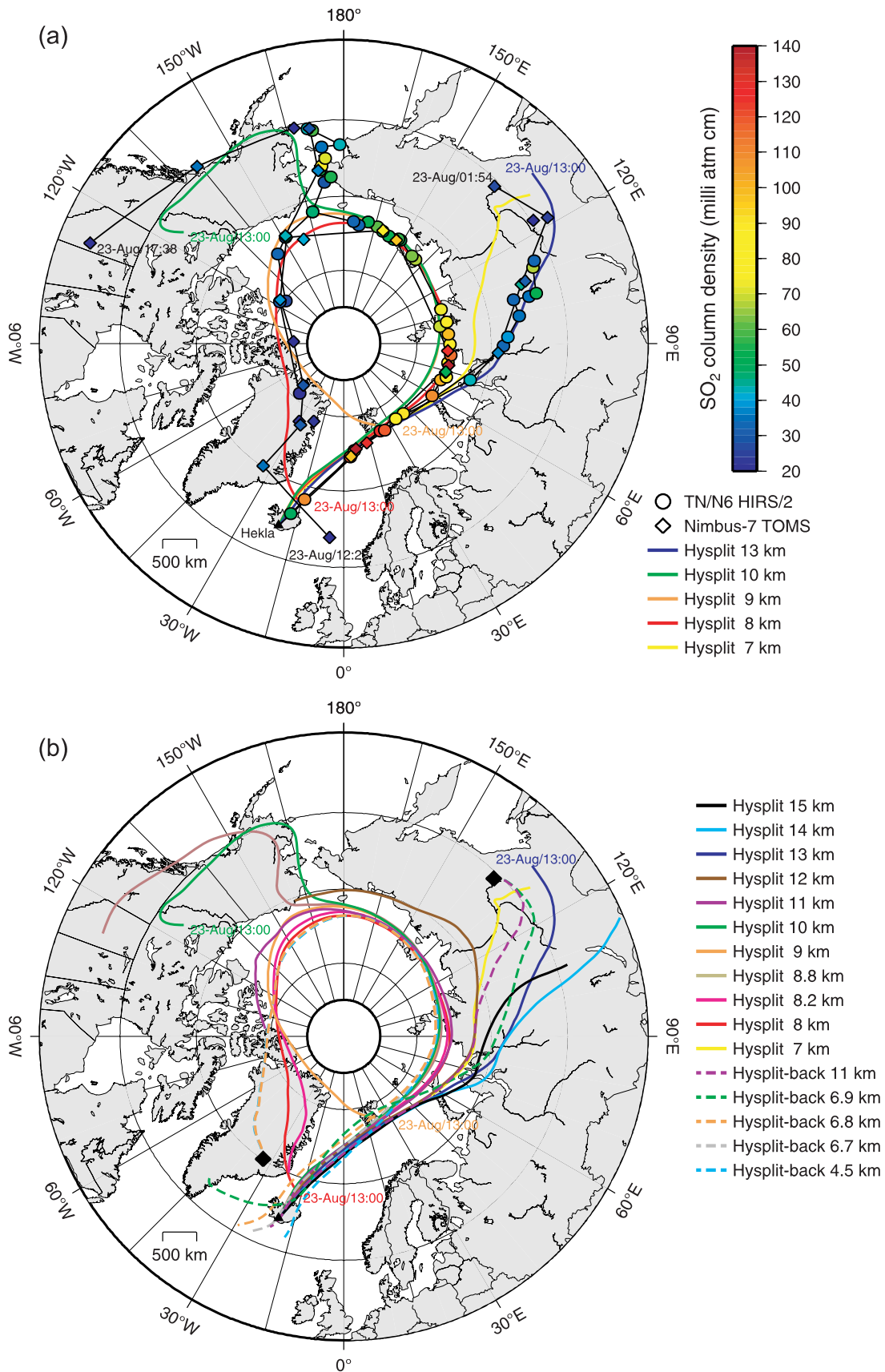


Figure 3

[22] HIRS/2 provided earlier observations than TOMS (Table 2; Figure 2), but those containing the entire SO₂ cloud were made prior to the end of the main emission phase (Table 2), precluding a measurement of the total erupted SO₂ burden. Total SO₂ burdens derived from HIRS/2 were lower than those from TOMS (Table 2), but this may be ascribed to differing sensitivity (see later discussion) and possibly to the smaller HIRS/2 swath width (Table 1). Although lava effusion continued at Hekla until August 20, no further emissions from the volcano were detected by TOMS or HIRS/2 after August 18.

[23] Around the time of its passage over Novaya Zemlya on August 19, the cloud split with one parcel observed drifting across central Russia whilst the remaining SO₂ continued to encircle the Arctic Ocean (Figures 1 and 2). The cloud that drifted across Russia was tracked by N7/TOMS until August 23 at 0154 UT, when it was located near the Sea of Okhotsk to the north of Sakhalin Island (Figure 1). HIRS/2 was able to track this portion of the cloud until 1141 UT on August 21 (Table 3). Comparison of HYSPLIT trajectories with the SO₂ data reveals that this cloud parcel reached the highest altitude attained by the 1980 eruption cloud (~13–15 km; Figure 3; see later discussion).

[24] Further separation of the SO₂ occurred as the cloud drifted north of Alaska on August 20. Perhaps under the influence of a depression over the Chukchi Sea, a parcel of SO₂ was advected across far eastern Russia and the Bering Sea and then across Alaska, directly over Anchorage (Figure 1). Numerous trans-Pacific air routes traverse this busy corridor, although we are not aware of any reported aviation encounters with the SO₂ cloud, in contrast to the long-lived 1991 Cerro Hudson eruption cloud that circled the southern hemisphere and caused several aviation encounters over Australia [Barton *et al.*, 1992]. The final N7/TOMS observation of the Hekla cloud that traversed Alaska occurred at 1738 UT on August 23 (>6 days after the eruption) over central Canada (Figure 1). HIRS/2 ceased detecting the cloud soon after the separation north of Alaska (Figure 2), but N7/TOMS tracked the residual SO₂ as it continued to circle the pole, drifting just north of Ellesmere Island and across north–east Greenland before the final TOMS observation at 1223 UT on August 23, when the elongate cloud straddled Iceland (Figure 1). Overall the SO₂ cloud was tracked for over 148 hours (~6.2 days) from the time of eruption.

[25] We are confident that other volcanic contributions to the observed SO₂ can be ruled out. The only other eruption detected by N7/TOMS in August 1980 was a small explosion from the lava dome at Mt St Helens on 7 August, which produced no measurable SO₂. An eruption of Bezymianny (Kamchatka) was reported on 21 August 1980 [Simkin and Siebert, 1994] but neither TOMS nor HIRS/2 detected any significant SO₂ emissions associated with this event.

4.2. Relationship to the Meteorological Environment

[26] We suggest that the overall pattern of SO₂ dispersal after the 1980 Hekla eruption, and the longevity of this modestly sized SO₂ cloud, can be at least partially ascribed to unusual synoptic activity in the Arctic Basin in August 1980. In contrast to the February 2000 winter eruption, which tracked across the Greenland Sea and Barents Sea under the influence of a strong low-pressure system before dispersing over eastern Russia [Rose *et al.*, 2003; Lacasse *et al.*, 2004; Höskuldsson *et al.*, 2007], a weakening or absence of the Icelandic Low in the summer of 1980 allowed the August 1980 SO₂ cloud to move further north and enter the Arctic Basin. Serreze and Barry [1988] report the migration of a cyclone into the Canada Basin on 16 August, and the persistence of this low until 11 September; deemed the most significant synoptic event of the 1979–1985 period. A strong upper air low persisted above the surface low for the lifetime of the disturbance, and pressure maps reproduced by Serreze and Barry [1988] indicate that the Hekla SO₂ cloud flowed around the cyclone until high pressure over Greenland altered its trajectory (Figure 1). We propose that the unusually stable Arctic weather pattern prevailing during transport of the Hekla volcanic cloud prolonged its lifetime by reducing any wind shear associated with migrating cyclones, analogous to the more stable polar vortex that forms over Antarctica in winter. The fragmentation of the SO₂ cloud over Novaya Zemlya and the Chukchi Sea may shed some light on the structure of the August 1980 cyclone at different pressure levels.

4.3. Trajectory Model Evaluation and Volcanic Cloud Altitude

[27] The location of the maximum SO₂ column retrieved by N7/TOMS and HIRS/2 in each orbit is used as a proxy for the cloud trajectory (Figure 3). Very little detectable ash was produced by the 1980 eruption, so the SO₂ data are a unique source of information on cloud movement and the high density of SO₂ retrievals achieved by combining the UV and IR measurements for this high latitude cloud allows a precise determination of its trajectory (Figure 3). Very good agreement is seen between selected HYSPLIT forward and backward trajectories and the path of the satellite-derived SO₂ maxima (Figure 3). The best fit trajectories correspond to altitudes of 13 km, 10 km and 8 km for the cloud segments that dispersed over eastern Russia, central Canada, and back over Iceland, respectively (Figure 3). Such altitudes are predominantly above the tropopause at the Arctic latitudes under consideration. It is clear from Figure 3 that the high density of SO₂ measurements improves the comparison between observed and model trajectories. For example, the HYSPLIT forward trajectory at 7 km altitude shown on Figure 3 provides a reasonably good match for the initial cloud trajectory and the final TOMS observation. However, consideration of the full set

Figure 3. (a) Peak SO₂ column amounts measured by N7/TOMS and TN/N6 HIRS/2 during atmospheric residence of the 1980 Hekla volcanic cloud, with best-fit HYSPLIT forward trajectories superimposed. Dates and times (UTC) of the final satellite observations and model trajectory end points are indicated. (b) An ensemble of HYSPLIT forward trajectories (*solid lines*) and back trajectories (*dashed lines*) for air parcels at various altitudes. Dates and times (UTC) of the best-fit model trajectory end points are indicated, as in (a). *Diamonds* indicate the start locations of the HYSPLIT back trajectories.

of satellite observations shows that the 13 km trajectory gives a much better fit for the cloud's entire path.

[28] We note that the 13 km maximum altitude derived here is lower than the 15 km altitude reported by observers of the eruption [Grönvold *et al.*, 1983], but accurate ground-based estimates of eruption column height can be difficult. However, since the HYSPLIT forward trajectories for altitudes of 13 km and 15 km coincide for at least the first ~24 hours posteruption, it is possible that the eruption cloud initially reached 15 km but later stabilized at 13 km. We also note that the timing of tephra fallout and the distribution of the tephra blanket over north Iceland was consistent with the transport of ash in a high velocity layer between 7 and 12 km altitude [Grönvold *et al.*, 1983], in good agreement with our inferred altitude range.

[29] Deviations between the HYSPLIT trajectories and the SO₂ cloud positions occur toward the trajectory end points (Figure 3), as no single forward trajectory altitude was found that provided a good fit with each cloud's entire path. This probably reflects changes in SO₂ cloud altitude during transport that were not captured by HYSPLIT. Since the trajectories for a range of altitudes are essentially identical for the initial stage of cloud transport, it is unclear if the SO₂ cloud was vertically extensive at the outset or if vertical segregation occurred later on under the influence of the meteorological environment. However, we consider it likely that the continuous emissions and tephra fall lasting several hours that were reported during the eruption [Grönvold *et al.*, 1983] produced a vertically extensive volcanic cloud, as the intensity of the eruption waxed and waned generating a plume with variable injection height.

5. Volcanic Cloud Composition

[30] The temporal evolution of SO₂ mass measured by TOMS in the volcanic clouds is shown in Figure 4. An increase in SO₂ burden around 80 hours after the eruption (Figure 4a) is apparent, and is also evident in HIRS/2 data (Table 4), though we believe this to be a result of varying retrieval conditions rather than a genuine mass increase (see later discussion). Exponential fits to the curves in Figure 4 yield SO₂ loss rates of 10^{-5} – 10^{-6} s⁻¹, which are typical of the UTLS. Loss rates appear slightly higher in the cloud portions that detached from the main cloud and moved south, probably due to increased rates of photochemistry at lower SZAs. Extrapolation of loss rates back to the time of eruption implies a total eruption mass of ~0.52–0.7 Tg SO₂, and consideration of the SO₂ mass contained in the detached clouds suggests that the higher figure is more realistic. This is in reasonable agreement with the 1980 eruption SO₂ yield estimated from petrological data (0.36 ± 1.2 Tg) [Sharma *et al.*, 2004]. For comparison, the 1991 Cerro Hudson eruption into the south polar stratosphere produced roughly three times more SO₂ than the 1980 Hekla eruption (~1.5 Tg), and was tracked for about three times longer [Schoeberl *et al.*, 1993].

[31] A sulfate aerosol signal (negative TOMS AI) is first apparent on 19 August at 0047 UT but it is generally much weaker than the AI signal for the February 2000 eruption cloud [Rose *et al.*, 2003]. The absence of a significant sulfate aerosol signal in 1980, compared to the 2000 eruption, could indicate a drier atmosphere in 1980 relative

to 2000 (perhaps consistent with the absence of the Icelandic Low in 1980), and hence less entrainment of atmospheric water vapor [Glaze *et al.*, 1997]. Other possibilities are an influx of water vapor from the snowpack that covered the volcano during the 2000 winter eruption, or, less likely, a higher magmatic H₂O content in the magma erupted in 2000 (Höskuldsson *et al.* [2007] report a juvenile magmatic water content of 2.3 wt% for the 2000 eruption, and although we are unaware of any related data for the 1980 magma, this is a high value for a nonarc basalt [e.g., Wallace, 2005]. However, Sharma *et al.* [2004] report similar preeruptive sulfur contents (~900 ppm) in both magmas). A small negative AI (–1) can also indicate ice, which was probably more abundant in the February 2000 plume due to colder temperatures. Furthermore, the N7/TOMS AI is defined differently to the EP/TOMS AI; the former uses longer UV wavelengths and results in different AI signal strength for a given aerosol loading.

6. Comparison of TOMS and HIRS/2 Retrievals

6.1. Comparisons of SO₂ Burdens and Column Amounts

[32] Here we provide some initial comparisons between the TOMS and HIRS/2 SO₂ retrievals in the 1980 Hekla eruption cloud. A detailed comparison of the two data sets will be the subject of a separate paper, and will benefit from the trajectory analysis shown here as it will permit tuning of SO₂ retrievals (particularly from HIRS/2) for the most likely SO₂ vertical distribution. Prata *et al.* [2003] and Guo *et al.* [2004] report general agreement (5–30% differences) between total SO₂ burdens derived from HIRS/2 and TOMS for major volcanic SO₂ emissions such as the 1991 Pinatubo eruption cloud, with HIRS/2 values higher than TOMS. For the 1980 Hekla eruption, SO₂ burdens derived from HIRS/2 were nearly always lower than those derived from TOMS at around the same time (Tables 2, 3, and 4). We assume that this is partly a result of the narrower swath width of the HIRS/2 instrument (Table 1) and the frequent intersection of the TOVS calibration sequence (a data gap of 3 scan lines) with the SO₂ cloud. It is also likely that the sensitivity of the HIRS/2 SO₂ retrieval was often limited by thermal contrast (e.g., as the SO₂ cloud drifted over Arctic sea ice; Figure 5), the thickness of the SO₂ cloud (likely to be thinner at the cloud margins) and the occurrence of meteorological clouds, although elaboration of these effects is not possible without further information on contemporary meteorology and ground cover. Altitude effects on the IR retrievals are also significant; Prata *et al.* [2003] indicate an absorber amount error on the order of 5–10% for a ±1 km error in SO₂ cloud height assignment. Here the maximum difference between the SO₂ layer altitude assumed in HIRS/2 retrievals (11 km) and the altitude estimated from trajectory modeling (8–15 km) is 3–4 km, indicating potential errors of 15–40%.

[33] Figures 1, 2, and 3 show that the modeled trajectory and observed transport of SO₂ in the Hekla volcanic cloud are in good general agreement. At the level of individual satellite footprints, comparison between the TOMS and HIRS/2 retrievals is more complex, as the measured SO₂ column amounts are affected by the scan position of each observation, and partial coverage of the cloud by HIRS/2

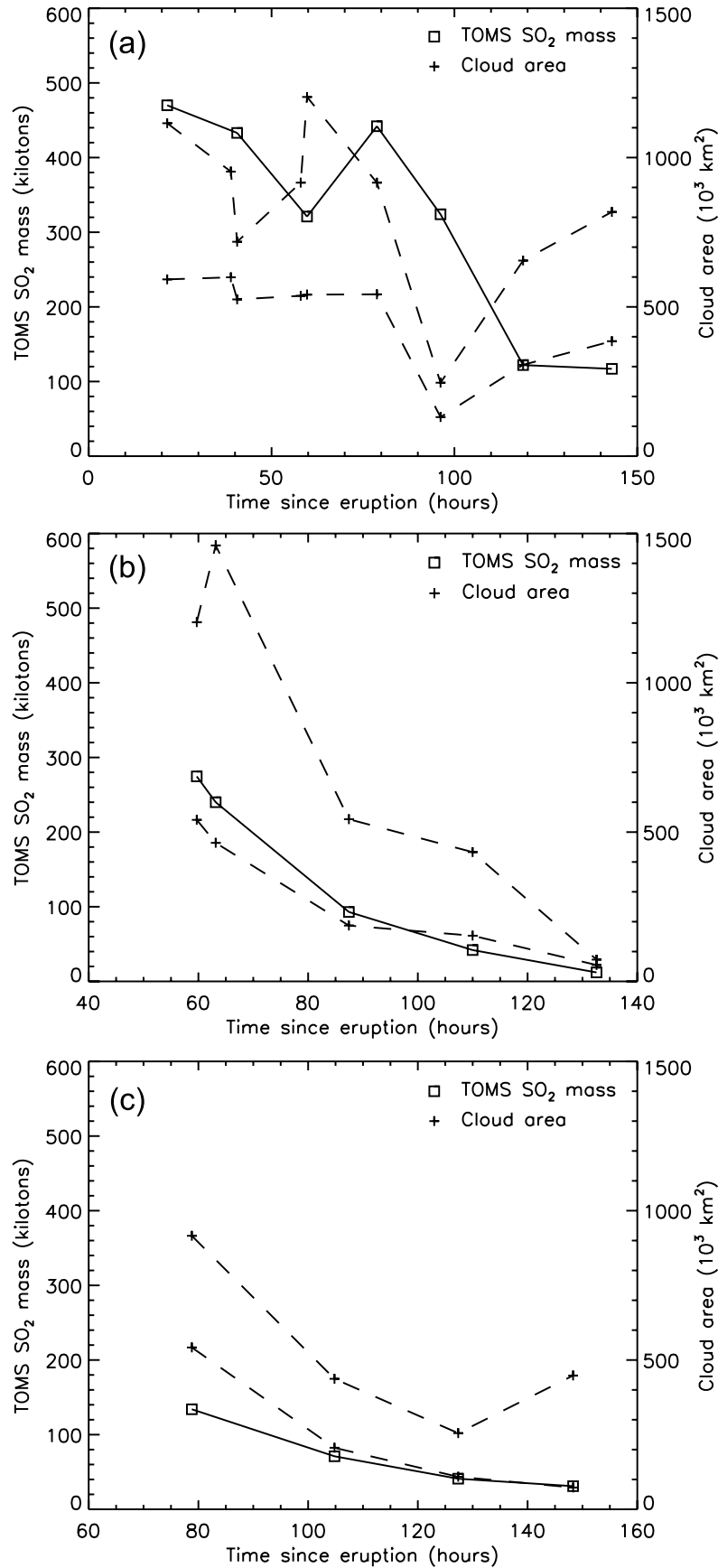


Figure 4

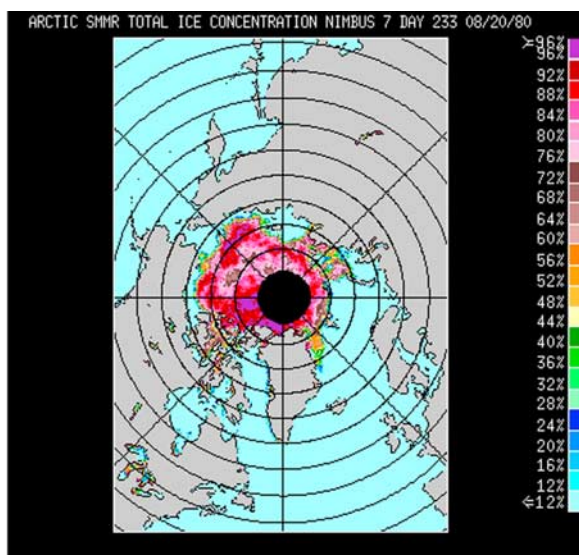


Figure 5. Arctic sea ice concentrations (in %) on 20 August 1980, derived from the Nimbus-7 Scanning Multi-channel Microwave Radiometer (SMMR) [Cavaliere *et al.*, 2004].

was common (i.e., the most concentrated region of the cloud was rarely observed by both sensors near simultaneously). Typically, higher SO₂ columns will be measured in near-nadir FOVs for subpixel sized clouds due to averaging effects. If SO₂ fills the satellite FOV at all scan angles, then measured column amounts should be similar across the swath. For this reason we choose to compare TOMS and HIRS/2 retrievals where the highest SO₂ columns were measured (Tables 2, 3, and 4), as we presume the SO₂ cloud covered the entire sensor FOV at these locations.

[34] The smallest time difference between TOMS and HIRS/2 overpasses (~ 1 minute) occurred on 19 August at 02:30–02:31 UT when the SO₂ cloud straddled northern Novaya Zemlya (Figures 1 and 2). HIRS/2 only captured the eastern end of the cloud whilst TOMS provided almost complete coverage, and perhaps as a result the maximum TOMS SO₂ column (129 DU) exceeded that of HIRS/2 (75 DU), although the locations of the maxima are similar (Table 2). Scan position effects may be significant as the HIRS/2 measurement was at the edge of the scan (scan position 56) whereas the TOMS observation was near nadir (scan position 26). However, biases in the retrievals cannot be ruled out. Another closely spaced pair of observations occurred at 05:51 (HIRS/2) and 05:56 UT (TOMS) on 19 August, just north of the Russian mainland. Peak SO₂ columns measured by TOMS (136 DU) and HIRS/2 (114 DU) differ but are within the error bounds discussed previously, and the locations of the maxima are similar (Table 2). Also, both sensors observed the cloud at similar,

moderately off-nadir scan angles (Table 2). We also note very good agreement (within error) between the location and magnitude of TOMS and HIRS/2 maximum SO₂ columns on 18 August at 07:23 UT (TOMS; 107 DU, off nadir) and 07:57 UT (HIRS/2; 119 DU, off nadir), when the cloud was SW of Svalbard and relatively compact (Table 2), despite the larger time difference (34 minutes). Our preliminary conclusion is that the two retrievals are in good agreement when observing the same cloud mass in a similar geometrical configuration under optimum environmental conditions (which differ for TOMS and HIRS/2), but that such situations are rare, even in a seemingly favorable case such as this.

[35] For the volcanic cloud that circled the North Pole, most of the favorable comparisons between TOMS and HIRS/2 occur relatively early in its lifetime. Later in the evolution of the cloud, maximum SO₂ columns retrieved using TOMS are typically higher than (by up to 100%) the closest available HIRS/2 columns (Table 2; e.g., note the sequence of measurements between 18:25 and 20:08 UT on 20 August). It is interesting to note that this is contrary to the observations of Guo *et al.* [2004] for the 1991 Pinatubo SO₂ cloud. They remarked that the difference between HIRS/2 and TOMS maximum SO₂ columns increased with time, with the HIRS/2 columns up to 40–50% higher than corresponding TOMS columns, 370 hours after the eruption [Guo *et al.*, 2004]. This was attributed to sulfate aerosol formation in the aging cloud, resulting in a positive bias in the HIRS/2 retrievals due to sulfate absorption in the 7.3 μm IR region, whilst the UV TOMS retrievals were unaffected [Guo *et al.*, 2004].

[36] Although the 1980 Hekla volcanic cloud was much shorter lived than the Pinatubo cloud, the high abundance of sulfate reported in Hekla emissions [Cadle and Blifford, 1971; Rose *et al.*, 2003; Hunton *et al.*, 2005] suggests that similar effects might be expected here. However, our results, while not conclusive, indicate the opposite. In the Hekla case we contend that sulfate aerosol (if present) may promote a positive bias in the TOMS retrievals due to UV scattering, which would increase photon path lengths through the SO₂ cloud, and which would be exacerbated at the high SZAs encountered during the entire lifetime of the cloud [Krueger *et al.*, 1995]. The precise effect of sulfate aerosol on UV and IR retrievals is dependent on aerosol composition and particle size, and may therefore vary with eruptive and environmental conditions. We also admit that altitude effects on the HIRS/2 retrievals may also contribute to the observed biases, given that an underestimate of the SO₂ cloud altitude will result in an underestimate of the SO₂ column [Prata *et al.*, 2003]. However, if cloud altitude were the major factor this would imply a more significant TOMS overestimate in the SO₂ cloud at higher altitude (the portion that drifted over Russia), which is not supported by our data (Table 3).

Figure 4. Temporal evolution of SO₂ burdens and cloud area for the 1980 Hekla volcanic cloud, derived from N7/TOMS data. Two cloud area estimates are shown in each plot using different background SO₂ offsets to isolate the volcanic signal [Krueger *et al.*, 1995]: the lower curve is derived using a constant SO₂ background of 15 DU; the upper curve uses the mean SO₂ amount observed in background regions in each TOMS scene. (a) SO₂ burdens for the main portion of the cloud that circumnavigated the Arctic Ocean. (b) SO₂ burdens for the cloud that traversed Russia. (c) SO₂ burdens for the cloud that traversed Alaska and Canada.

6.2. Observation and Interpretation of an Increase in SO₂ Cloud Mass

[37] An enigmatic feature of the Hekla volcanic cloud is an apparent increase ($\sim 30\%$) in SO₂ burden around 80 hours after the eruption at $\sim 20:00$ UT on 20 August (Figure 4a), when the cloud was located in the region of the Chukchi Sea north of Alaska and far-eastern Russia, and its leading edge was approaching Ellesmere Island (Figures 1 and 2). Although HIRS/2 SO₂ burdens are lower due to incomplete coverage of the cloud (and perhaps also due to generally lower retrieved SO₂ columns as discussed above), they show a similar pattern, and SO₂ column amounts also show an increase at the same time (Figure 2; Table 4). Previous TOMS volcanic cloud studies have shown SO₂ mass increases on the second day following eruptions, which has commonly been attributed to eruptive emissions of H₂S which oxidize to SO₂ after emission [Bluth *et al.*, 1995; Constantine *et al.*, 2000; Rose *et al.*, 2000]. Guo *et al.* [2004] implicated the release of SO₂ from a sublimating ice-gas mixture to explain an observed SO₂ mass increase in the 1991 Pinatubo volcanic cloud 55–70 hours after the eruption. Given the timescale of the mass increase we observe for the Hekla cloud, the latter explanation seems plausible. However, below we posit another explanation involving a change in the measurement conditions at the time of the observed mass increase.

[38] In our view a more likely reason for the SO₂ enhancement is the passage of the cloud over a region of sea ice as it moved north of Alaska. The presence of sea ice in the northern Chukchi Sea and East Siberian Sea at this time is supported by NOAA maps of minimum sea ice extent for 20 August 1980 (Figure 5). Although the sea ice map (Figure 5) indicates that the SO₂ cloud also passed over ice-covered regions earlier on, it appears that the TOMS observation on 20 August at 20:08 UT occurred when sea ice underlay a significant fraction ($\sim 70\%$) of the SO₂ cloud. Where underlying sea ice enhances surface reflectivity the TOMS algorithm could overestimate SO₂ columns by 50% in a cloud located at 10 km altitude [Krueger *et al.*, 1995], which would account for the observations. Indeed, the subsequent passage of the cloud over sea ice in the Canadian Arctic and over the Greenland ice cap is probably the main reason for its prolonged detection by TOMS. The cause of the mass increase measured by HIRS/2 on 20 August is less clear. Inspection of the HIRS/2 retrievals shows that the SO₂ enhancement occurs over the southern Chukchi Sea and Bering Strait, south of the sea ice limit in Figure 5 and in a different location to the enhancement measured by TOMS. Surface reflectivity has no influence in the IR, but a drying of the atmosphere or a decrease in thermal contrast would affect the IR retrievals (resulting in detection of more and less SO₂, respectively), as would inadequate knowledge of plume altitude (detection of more SO₂ would imply an overestimate of the cloud altitude). Thus in the case of HIRS/2 it appears that the SO₂ enhancement is probably of environmental origin; a drier atmosphere and/or a decrease in the altitude of the SO₂ plume, probably linked to the fragmentation of the SO₂ cloud over the Chukchi Sea.

[39] As an addendum to this discussion we also stress that a chemical origin for the increase in SO₂ mass cannot be ruled out. Petrological studies have suggested that the Hekla

eruption in February 2000 emitted significant quantities of reduced sulfur species (H₂S and S₂) [Moune *et al.*, 2007] in addition to the SO₂ measured by remote sensing [Rose *et al.*, 2003]. We assume that this could also apply to the 1980 eruption as Hekla eruptions since 1970 have been compositionally quite uniform [Moune *et al.*, 2007; Höskuldsson *et al.*, 2007]. The average lifetime of H₂S in the lower atmosphere is 2 days [Lelieveld *et al.*, 1997], but significant variation has been reported [Bowyer, 2003; Aiuppa *et al.*, 2005]: from less than 1 day in polluted air to 42 days in winter at high latitudes [Bottenheim and Strausz, 1980]. This is because H₂S is relatively insoluble and oxidation usually proceeds via reaction with OH radicals in the gas phase, and is therefore dependent on the abundance of OH and homogeneous reaction rates [Cox and Sheppard, 1980], and hence solar exposure. Thus at the high latitudes of the 1980 Hekla eruption cloud it is possible that the H₂S lifetime exceeded 1–2 days, and therefore oxidation of H₂S could possibly explain the SO₂ mass increase observed on 20 August, ~ 3 –4 days after the eruption. However, if significant H₂S is expected in Hekla emissions, and its mean lifetime is 2 days, then it is surprising that H₂S was not detected in the February 2000 Hekla cloud when it was directly sampled by a NASA DC8 33–34 hours after the eruption [Hunton *et al.*, 2005; Rose *et al.*, 2006]. Rose *et al.* [2006] concluded that the volcanic H₂S had been oxidized by that time, indicating a shorter than average lifetime. Thus it is clear that significant ambiguity persists regarding the fate of H₂S in volcanic clouds, which requires further investigation.

7. Volcanological Significance

[40] The total SO₂ emission of ~ 0.5 – 0.7 Tg measured in the 17 August 1980 cloud is over twice that determined for the 26 February 2000 eruption of Hekla by HIRS/2 (~ 0.2 Tg) [Rose *et al.*, 2003], even if the lower bound of our 1980 eruption SO₂ loading is used. However, uncertainty remains over the magnitude of SO₂ emissions in 2000. Recent petrological analyses imply a possible total SO₂ release of 0.6–3.8 Tg (Table 5), with a significant fraction derived from oxidation of reduced sulfur species (such as H₂S) that are invisible to satellite remote sensing [Moune *et al.*, 2007], although others have reported lower petrological SO₂ yields (0.48 ± 0.14 Tg) [Sharma *et al.*, 2004]. Remote sensing of the volcanic cloud in 2000 was also hampered by the winter season and high latitude (in the case of TOMS) and by poor thermal contrast as the cloud drifted over the Greenland ice cap (in the case of HIRS/2 and MODIS) [Rose *et al.*, 2003]. We are confident that these latter factors were negligible for the 1980 eruption and that our SO₂ loading measurement is accurate. However, in both eruptions, scavenging of gases by absorption onto tephra, condensation onto snow, and trapping in icy hydrometeors removed some sulfur species from the plume [Moune *et al.*, 2007], as was observed in the 1970 Hekla eruption [Calle and Blifford, 1971]. Given these uncertainties, it is indeed possible that the SO₂ yield in 1980 and 2000 was similar. Erupted volumes of lava are easier to measure and have been remarkably consistent for Hekla's eruptions since 1970 (~ 0.2 km³, with the exception of the minor 1981 eruption; Table 5), although Höskuldsson *et al.* [2007] note that pre-

Table 5. Summary of Historical Hekla Eruptions Since 1947

Eruption Date	VEI ^a	Lava Volume (km ³)	Tephra Volume (km ³)	SO ₂ Emission (Tg)	Max. Plume Altitude (km)	References ^b
29 Mar 1947	4	0.80	0.21	– ^c	27	1, 2
5 May 1970	3	0.21	0.066	– ^d	16	1, 3
17 Aug 1980	3	0.15	0.058	0.5–0.7	13–15	1, 4, 5
9 Apr 1981	2	0.03	–	~0.01	6.6	1, 4, 6
17 Jan 1991	3	0.15	0.02	0.3–0.5	11.5	1, 6, 7
26 Feb 2000	3	0.189	0.01	0.1–0.4 ^e , 0.6–3.8 ^f	11–12	1, 8, 9, 10

^aVolcanic Explosivity Index [Newhall and Self, 1982].

^b1: *GVN* [2008]; 2: *Thorarinsson* [1967]; 3: *Thorarinsson and Sigvaldason* [1972]; 4: *Grönvold et al.* [1983]; 5: this work; 6: S.A. Carn, unpublished data; 7: *Gudmundsson et al.* [1992]; 8: *Höskuldsson et al.* [2007]; 9: *Rose et al.* [2003]; 10: *Lacasse et al.* [2004].

^cNo estimate of SO₂ emissions available, although a sulfate spike (and glass shards) correlated with the 1947 Hekla eruption have been reported in ice cores from the Yukon Territory, northern Canada [*Yalcin et al.*, 2003, 2007].

^dNo estimate of SO₂ emissions available, although a sulfate spike in the GISP2 Greenland ice core has been linked with this eruption [*Zielinski et al.*, 1994]. Notably, no sulfate spike associated with the 1947 eruption of Hekla has been found in GISP2.

^eSO₂ emissions measured by satellite remote sensing.

^fSO₂ emissions inferred from petrological analyses.

2000 eruption volumes could be underestimated due to insufficient knowledge of preeruption topography. SO₂ production also appears to have been of a similar magnitude for all recent Hekla eruptions (except 1981; Table 5). No estimates of SO₂ emissions currently exist for the 1947 and 1970 eruptions of Hekla, but sulfate spikes in ice cores provide evidence that substantial emissions of sulfur did occur (Table 5).

[41] The consistency of magmatic and gaseous output in recent Hekla eruptions supports a common eruptive process. It is widely acknowledged that Hekla eruptions are fed by dykes that propagate rapidly from depth [e.g., *Linde et al.*, 1993; *Soosalu et al.*, 2005], and the mechanism and associated geophysical signals are sufficiently well understood that eruptions can be predicted with some confidence [*Soosalu et al.*, 2005]. Precursory activity is confined to the 25–80 minutes before eruption, but the rise of a magma-filled dyke from depth within this timeframe requires unrealistically rapid ascent rates [*Soosalu and Einarsson*, 2004]. For the 1991 eruption, *Linde et al.* [1993] placed Hekla's magma chamber at 4–9 km depth, whereas *Soosalu et al.* [2005] found no evidence for a voluminous chamber above 14 km depth. Deformation after the 1980–81 eruption implied a magma chamber depth of ~8 km [*Kjartansson and Grönvold*, 1983]. An alternative explanation discussed by *Soosalu and Einarsson* [2004] is that Hekla eruptions are triggered by overpressure exerted by accumulated gases in the upper part of a deep magma reservoir. Hence the pressurized gases ascend rapidly and drive the initial phase of the eruption, followed by the magma, consistent with observations of Hekla's recent eruptions that have involved explosive venting of gases and tephra followed by effusion of lava flows [*Grönvold et al.*, 1983; *Gudmundsson et al.*, 1992; *Höskuldsson et al.*, 2007].

[42] A brief phase of precursory activity is also predicted by the model of *Menand and Tait* [2001] for basaltic eruptions driven by a propagating dyke. Analogue modeling of a liquid-filled crack with a gas pocket at its tip by *Menand and Tait* [2001] revealed that, once overpressure within the gas pocket has fractured the surrounding rock, the rising gases can separate from the liquid. Thus the gases breach the surface prior to the arrival of the liquid, as observed in Hekla's eruptions. Such a process could explain the gas-rich and ash-poor nature of Hekla's initial eruption

clouds (as we observe in the 1980 eruption), and might limit the amount of fine ash lofted to high altitudes, since the separation of gas from magma during ascent from depth would result in less magma fragmentation at the surface, and instead promote the effusion of relatively degassed lava flows. Based on such a model, we might expect the time delay between the initial gas-rich plume and subsequent lava flow effusion to scale with the depth from which the dyke propagates. We also note that little evidence has been found thus far for any sulfur excess in Hekla eruptions, including the 1980 eruption [*Sharma et al.*, 2004], implying that most or all of the magma supplying the measured SO₂ emissions is ultimately erupted.

8. Discussion

[43] Comparison of the 1980 eruption with other recent Hekla eruptions highlights the importance of the prevailing synoptic meteorology in controlling the trajectory of the volcanic plume. Specifically, the phase of the North Atlantic Oscillation (NAO) appears to be critical. The NAO is the dominant mode of natural climate variability in the North Atlantic region and is characterized by fluctuations in sea-level pressure difference between the Icelandic Low and the Azores High. Depending on the NAO reconstruction used, in August 1980 the NAO index was either close to zero or negative (0.3 or –2.49) [*Trenberth and Paolino*, 1980; *Jones et al.*, 1997] and, as shown here, a weak or absent Icelandic Low allowed the volcanic cloud to move further north and impact the Arctic basin. In contrast, the NAO index in February 2000 was strongly positive (4.37 or 2.75) [*Trenberth and Paolino*, 1980; *Jones et al.*, 1997], indicating a dominant Icelandic Low that prevented the Hekla volcanic cloud from penetrating the Arctic Basin. Similarly, the NAO index was positive during the January 1991 Hekla eruption [*Trenberth and Paolino*, 1980; *Jones et al.*, 1997] and the emitted SO₂ cloud tracked eastward across central Russia. In May 1970 the NAO index was also positive [*Trenberth and Paolino*, 1980; *Jones et al.*, 1997]. Initial tephra dispersal was NNW of Hekla [*Thorarinsson and Sigvaldason*, 1972] and a sulfate peak in the Greenland GISP2 ice core has been linked to this eruption [*Zielinski et al.*, 1994], but we have no other information on long-range transport of the volcanic plume. During the March

1947 eruption the NAO index was negative [Trenberth and Paolino, 1980; Jones et al., 1997], and although tephra fall occurred south of Hekla and over Scandinavia [Thorarinsson, 1967], related horizons in ice cores from the Yukon Territory of Canada (Table 5) [Yalcin et al., 2003, 2007] suggest that the track of the 1947 eruption cloud may have been similar to the 1980 cloud trajectory.

[44] Given the remarkable 9–10 year periodicity of Hekla's recent eruptions (Table 5), the next eruption might be expected to occur sometime in 2009–2010. However, prediction of the NAO index is likely to be more difficult than forecasting of the eruption due to noise in the NAO signal. As of 2006/2007 the winter NAO was positive and a general downward trend has been noted since the early 1990s (available at http://www.cru.uea.ac.uk/~timo/projpages/nao_update.htm) [Osborn, 2006].

[45] The Arctic cyclone that controlled the trajectory of the 1980 volcanic cloud could be considered as analogous to the more stable lower stratospheric polar vortex that forms during the winter. Polar vortices contain regions of highly isolated air, with exchange of trace gases occurring primarily at the vortex edge via the action of erosional waves [Schoeberl et al., 1992]. This appears consistent with our measurements of the Hekla SO₂ cloud, which track parcels of SO₂ splitting from the main cloud at the edge of the cyclone, perhaps due to depressions (polar lows) over the Chukchi Sea and Siberia. Hence the trajectory of this unique volcanic cloud may provide some insight into the erosion of polar vortices or Arctic cyclonic systems, providing further evidence for the value of SO₂ as a tracer of UTLS dynamics [e.g., Schoeberl et al., 1993]. Since atmospheric dynamics in the Arctic are more variable than in the Antarctic, tracer studies such as that presented here could support more accurate models.

[46] The Arctic polar vortex is less stable than its Antarctic equivalent, owing to the different configuration of ocean and landmasses at each pole. As a result, temperatures are lower in the Antarctic vortex, permitting formation of polar stratospheric clouds (PSCs) that catalyze ozone destruction [Seinfeld and Pandis, 2006]. The threshold temperature for PSC formation is -78°C [McCormick et al., 1982]. Significant Arctic ozone loss only occurs following winters characterized by particularly cold polar stratospheric temperatures [e.g., Salawitch et al., 1993]. An Arctic ozone hole became apparent in the 1990s due to cooling stratospheric temperatures, and ozone loss promotes further cooling due to a reduction in radiative warming [e.g., Randel and Wu, 1999]. High volcanic aerosol loading in the Arctic stratosphere following Hekla eruptions could promote significant ozone loss via heterogeneous reactions. This is partly because volcanic aerosol can promote stratospheric denitrification, a requirement for efficient ozone depletion, even if temperatures are not low enough for PSC formation [Seinfeld and Pandis, 2006]. Arctic ozone loss is a concern as it could potentially expose large populations in northern Europe and Asia to high UV doses.

[47] Hekla is one of the most northerly active volcanoes that produce frequent explosive eruptions. There is thus considerable potential for Arctic ozone loss after Hekla eruptions, depending on the trajectory of the plume. Using in situ measurements from a NASA DC8 aircraft, Rose et al.

[2006] contend that ozone destruction occurred in the February 2000 eruption cloud, catalyzed by the formation of volcanogenic PSCs within the volcanic cloud at temperatures of 201–203 K. Furthermore, the in situ data suggest limited scavenging of halogen species such as HCl [Rose et al., 2006], indicating substantial stratospheric injection of chlorine. However, the 2000 eruption occurred in winter with correspondingly colder stratospheric temperatures. We expect less significant ozone loss occurred following the 1980 eruption due to higher temperatures, although it remains a possibility owing to the significant volcanic aerosol injection and long residence time of the cloud, coupled with solar exposure to promote photolytic reactions. However, any ozone depletion is likely to be localized and of small magnitude and therefore not measurable with N7/TOMS.

9. Summary

[48] The August 1980 eruption of Hekla injected a substantial amount of SO₂ (0.5–0.7 Tg) into the Arctic stratosphere. We have used TOMS and HIRS/2 SO₂ retrievals to track the cloud as it circled the North Pole and segmented over Siberia and the Chukchi Sea, apparently under the influence of an unusually persistent cyclone in the Arctic Basin. This trajectory is unique in the 30-year history of UV and IR satellite remote sensing of volcanic clouds. Trajectory modeling using HYSPLIT indicates that the SO₂ cloud occupied an altitude range between 8 and 15 km. Although the high latitude of the 1980 Hekla SO₂ cloud is favorable for comparisons between UV and IR retrievals of SO₂, these comparisons are complicated by differing sensor geometries, algorithm sensitivities and environmental conditions. However, we find that TOMS and HIRS/2 SO₂ retrievals agree within error for near-coincident FOVs with similar geometries. Procedures for a more rigorous comparison of TOMS and HIRS/2 retrievals are under development. Ascertaining the cloud altitude is of fundamental importance when comparing independent SO₂ retrievals. We have shown that this can be effectively achieved using a combination of trajectory modeling and frequent SO₂ measurements.

[49] If the recent cooling trend in the Arctic stratosphere continues, future explosive eruptions of Icelandic volcanoes such as Hekla, particularly in the late winter or spring, could play a significant role in promoting Arctic ozone loss. Hekla eruptions have become more frequent since 1970 and follow a pattern of early explosive venting of volcanic gases, with significant stratospheric injection. The phase of the NAO prevailing at the time of the eruption appears to strongly influence the trajectory of volcanic clouds from Hekla.

[50] **Acknowledgments.** This work was supported by NASA through funding of the TOMS Science Team. We thank three reviewers for constructive comments on the paper. The NOAA Air Resources Laboratory (ARL) is acknowledged for the provision of the HYSPLIT model and READY website (available at <http://www.arl.noaa.gov/ready.html>) used in this publication.

References

- Aiuppa, A., S. Inguaggiato, A. J. S. McGonigle, M. O'Dwyer, C. Oppenheimer, M. J. Padgett, D. Rouwet, and M. Valenza (2005), H₂S fluxes from Mt. Etna, Stromboli, and Vulcano (Italy) and implications for the sulfur budget at volcanoes, *Geochim. Cosmochim. Acta*, 69(7), 1861–1871.

- Barton, I. J., A. J. Prata, I. G. Watterson, and S. A. Young (1992), Identification of the Mount Hudson volcanic cloud over SE Australia, *Geophys. Res. Lett.*, *19*, 1211–1214.
- Bluth, G. J. S., C. C. Schnetzler, A. J. Krueger, and L. S. Walter (1993), The contribution of explosive volcanism to global atmospheric sulfur dioxide concentrations, *Nature*, *366*, 327–329.
- Bluth, G. J. S., C. J. Scott, I. E. Sprod, C. C. Schnetzler, A. J. Krueger, and L. S. Walter (1995), Explosive emissions of sulfur dioxide from the 1992 Crater Peak eruptions, Mount Spurr volcano, Alaska, in *The 1992 eruptions of Crater Peak Vent, Mount Spurr volcano, Alaska*, edited by T. E. C. Keith, *U.S. Geol. Surv. Bull.*, *2139*, 37–45, US Government Printing Office, Washington, D.C.
- Bottenheim, J. W., and O. P. Strausz (1980), Gas phase chemistry of clean air at 55°N latitude, *Environ. Sci. Technol.*, *14*, 709–718.
- Bowyer, J. (2003), Residence time for hydrogen sulfide in the atmosphere literature search results, North Carolina Department of Environment and Natural Resources, Division of Air Quality. (Available at http://daq.state.nc.us/toxics/studies/H2S/H2S_Ambient_Air.pdf)
- Cadle, R. D., and I. H. Blifford (1971), Hekla eruption clouds, *Nature*, *230*, 573–574.
- Carn, S. A., D. J. Schneider, G. J. S. Bluth, S. E. Kobs, W. I. Rose, and G. G. Ernst (2002), On the separation of ash and sulfur dioxide in volcanic clouds, *Eos Trans. AGU*, *83*(19), Spring Meet. Suppl., Abstract V51A-03.
- Cam, S. A., A. J. Krueger, G. J. S. Bluth, S. J. Schaefer, N. A. Krotkov, I. M. Watson, and S. Datta (2003), Volcanic eruption detection by the Total Ozone Mapping Spectrometer (TOMS) instruments: A 22-year record of sulphur dioxide and ash emissions, in *Volcanic Degassing, Spec. Publ. Geol. Soc. Lon.*, vol. 213, edited by C. Oppenheimer, D. M. Pyle, and J. Barclay, pp. 177–202, Geol. Soc., London, U.K.
- Carn, S. A., L. L. Strow, S. de Souza-Machado, Y. Edmonds, and S. Hannon (2005), Quantifying tropospheric volcanic emissions with AIRS: The 2002 eruption of Mt. Etna (Italy), *Geophys. Res. Lett.*, *32*, L02301, doi:10.1029/2004GL021034.
- Carn, S. A., N. A. Krotkov, K. Yang, R. M. Hoff, A. J. Prata, A. J. Krueger, S. C. Loughlin, and P. F. Levelt (2007), Extended observations of volcanic SO₂ and sulfate aerosol in the stratosphere, *Atmos. Chem. Phys. Discuss.*, *7*, 2857–2871. (Available at <http://www.atmos-chem-phys-discuss.net/7/2857/2007/acpd-7-2857-2007.html>)
- Casadevall, T. J. (1994), The 1989–1990 eruption of Redoubt Volcano, Alaska; impacts on aircraft operations, *J. Volcanol. Geotherm. Res.*, *62*, 301–316.
- Cavalieri, D., C. Parkinson, P. Gloerson, and H. J. Zwally (2004), Sea ice concentrations from Nimbus-7 SMMR and DMSP SSM/I passive microwave data, August 1980. Boulder, Co: National Snow and Ice Data Center. Digital media.
- Constantine, E. K., G. J. S. Bluth, and W. I. Rose (2000), TOMS and AVHRR observations of drifting volcanic clouds from the August 1991 eruptions of Cerro Hudson, in *Remote Sensing of Active Volcanism, Geophys. Monogr. Ser.*, vol. 116, edited by P. J. Mouginiis-Mark et al., pp. 45–64, AGU, Washington, D. C.
- Cox, R. A., and D. Sheppard (1980), Reactions of OH radicals with gaseous sulphur compounds, *Nature*, *284*, 330–331.
- Draxler, R. R., and G. D. Rolph (2003), HYSPLIT (Hybrid Single-Particle Lagrangian Integrated Trajectory) Model access via NOAA ARL READY Website, NOAA Air Resources Laboratory, Silver Spring, MD. (Available at <http://www.arl.noaa.gov/ready/hysplit4.html>)
- Glaze, L. S., S. M. Baloga, and L. Wilson (1997), Transport of atmospheric water vapor by volcanic eruption columns, *J. Geophys. Res.*, *102*(D5), 6099–6108.
- Graf, H.-F., J. Feichter, and B. Langmann (1997), Volcanic sulfur emissions: estimates of source strength and its contribution to the global sulfate distribution, *J. Geophys. Res.*, *102*(D9), 10,727–10,738.
- Grindle, T. J., and F. W. Burcham Jr. (2002), Even minor ash encounters can cause major damage to aircraft, *ICAO J.*, *57*, 12–30.
- Grönvold, K., G. Larsen, P. Einarsson, S. Thorarinnsson, and K. Saemundsson (1983), The eruption of Hekla 1980–81, *Bull. Volcanol.*, *46*, 349–363.
- Gudmundsson, A., et al. (1992), The 1991 eruption of Hekla, Iceland, *Bull. Volcanol.*, *54*(3), 238–246.
- Guo, S., G. J. S. Bluth, W. I. Rose, I. M. Watson, and A. J. Prata (2004), Re-evaluation of SO₂ release of the 15 June 1991 Pinatubo eruption using ultraviolet and infrared satellite sensors, *Geochem. Geophys. Geosyst.*, *5*, Q04001, doi:10.1029/2003GC000654.
- GVN (2008), Hekla eruptive history, *Smithsonian Institution Global Volcanism Program*, (available at <http://www.volcano.si.edu/world/volcano.cfm?vnum=1702-07=&volpage=erupt>) accessed 25 Jan.
- Höskuldsson, A., N. Óskarsson, R. Pedersen, K. Grönvold, K. Vogfjörð, and R. Ólafsdóttir (2007), The millennium eruption of Hekla in February 2000, *Bull. Volcanol.*, *70*, 169–182, doi:10.1007/s00445-007-0128-3.
- Hunton, D. E., et al. (2005), In-situ aircraft observations of the 2000 Mt. Hekla volcanic cloud: Composition and chemical evolution in the Arctic lower stratosphere, *J. Volcanol. Geotherm. Res.*, *145*, 23–34.
- IPCC (2001), *Climate Change 2001: The Scientific Basis, Contribution of Working Group I to the Third Assessment Report of the Intergovernmental Panel on Climate Change*, edited by J. T. Houghton et al., 944, Cambridge Univ. Press, UK. (Available at http://www.grida.no/climate/ipcc_tar/wg1/index.htm)
- Jones, P. D., T. Jónsson, and D. Wheeler (1997), Extension to the North Atlantic Oscillation using early instrumental pressure observations from Gibraltar and South–West Iceland, *Int. J. Climatol.*, *17*, 1433–1450. (Available at <http://www.cru.uea.ac.uk/cru/data/nao.htm>)
- Kjartansson, E., and K. Grönvold (1983), Location of a magma reservoir beneath Hekla volcano, Iceland, *Nature*, *301*, 139–141.
- Krueger, A. J., L. S. Walter, P. K. Bhartia, C. C. Schnetzler, N. A. Krotkov, I. Sprod, and G. J. S. Bluth (1995), Volcanic sulfur dioxide measurements from the total ozone mapping spectrometer instruments, *J. Geophys. Res.*, *100*(D7), 14,057–14,076.
- Krueger, A. J., S. J. Schaefer, N. Krotkov, G. Bluth, and S. Barker (2000), Ultraviolet remote sensing of volcanic emissions, in *Remote Sensing of Active Volcanism, Geophys. Monogr. Ser.*, vol. 116, edited by P. J. Mouginiis-Mark, J. A. Crisp, and J. H. Fink, pp. 25–43, AGU, Washington, D. C.
- Lacasse, C., S. Karlsdóttir, G. Larsen, H. Soosalu, W. I. Rose, and G. G. J. Ernst (2004), Weather radar observations of the Hekla 2000 eruption cloud, Iceland, *Bull. Volcanol.*, *66*, 457–473, doi:10.1007/s00445-003-0329-3.
- Lelieveld, J., G.-J. Roelofs, L. Ganzeveld, J. Feichter, and H. Rodhe (1997), Terrestrial sources and distribution of atmospheric sulphur, *Phil. Trans. R. Soc. Lond. B*, *352*, 149–158.
- Linde, A. T., K. Ágústsson, I. S. Sacks, and R. Stefánsson (1993), Mechanism of the 1991 eruption of Hekla from continuous borehole strain monitoring, *Nature*, *365*, 737–740.
- McCormick, M. P., H. M. Steele, P. Hamill, W. P. Chu, and T. J. Swisler (1982), Polar stratospheric cloud sightings by SAM II, *J. Atmos. Sci.*, *39*(6), 1387–1397.
- McPeters, R. D., et al. (1996), Nimbus-7 Total Ozone Mapping Spectrometer (TOMS) Data Products User's Guide, *NASA Reference Publication 1384*, National Aeronautics and Space Administration, Washington, DC. (<http://macuv.gsfc.nasa.gov/doc/n7usrguide.pdf>)
- Menand, T., and S. R. Tait (2001), A phenomenological model for precursor volcanic eruptions, *Nature*, *411*, 678–680.
- Moune, S., O. Sigmarsson, T. Thordarson, and P.-J. Gauthier (2007), Recent volatile evolution in the magmatic system of Hekla volcano, Iceland, *Earth Planet. Sci. Lett.*, *255*, 273–289.
- Newhall, C. G., and S. Self (1982), The volcanic explosivity index (VEI): An estimate of explosive magnitude for historical volcanism, *J. Geophys. Res.*, *87*, 1231–1238.
- Osborn, T. J. (2006), Recent variations in the winter North Atlantic Oscillation, *Weather*, *61*, 353–355.
- Pieri, D., C. Ma, J. J. Simpson, G. Hufford, T. Grindle, and C. Grove (2002), Analyses of *in-situ* airborne volcanic ash from the February 2000 eruption of Hekla volcano, Iceland, *Geophys. Res. Lett.*, *29*(16), 1772, doi:10.1029/2001GL013688.
- Prata, A. J., and C. Bernardo (2007), Retrieval of volcanic SO₂ column abundance from Atmospheric Infrared Sounder data, *J. Geophys. Res.*, *112*, D20204, doi:10.1029/2006JD007955.
- Prata, A. J., S. Self, W. I. Rose, and D. M. O'Brien (2003), Global, long-term sulphur dioxide measurements from TOVS data: A new tool for studying explosive volcanism and climate, in *Volcanism and the Earth's Atmosphere, Geophys. Monogr. Ser.*, vol. 139, edited by A. Robock and C. Oppenheimer, pp. 75–92, AGU, Washington, D. C.
- Randel, W. J., and F. Wu (1999), Cooling of the Arctic and Antarctic polar stratospheres due to ozone depletion, *J. Climate*, *12*(5), 1467–1479.
- Rolph, G. D. (2003), Real-time Environmental Applications and Display system (READY) Website, NOAA Air Resources Laboratory, Silver Spring, Md. (Available at <http://www.arl.noaa.gov/ready/hysplit4.html>)
- Rose, W. I., D. J. Delene, D. J. Schneider, G. J. S. Bluth, A. J. Krueger, I. Sprod, C. McKee, H. L. Davies, and G. G. J. Ernst (1995), Ice in the 1994 Rabaul eruption cloud: Implications for volcano hazard and atmospheric effects, *Nature*, *375*, 477–479.
- Rose, W. I., G. J. S. Bluth, and G. G. J. Ernst (2000), Integrating retrievals of volcanic cloud characteristics from satellite remote sensors: A summary, *Phil. Trans. R. Soc. Lond. A*, *358*, 1585–1606.
- Rose, W. I., et al. (2003), The February–March 2000 eruption of Hekla, Iceland from a satellite perspective, in *Volcanism and the Earth's Atmosphere, Geophys. Monogr. Ser.*, vol. 139, edited by A. Robock and C. Oppenheimer, pp. 107–132, AGU, Washington, D. C.
- Rose, W. I., et al. (2006), Atmospheric chemistry of a 33–34 hour old volcanic cloud from Hekla volcano (Iceland): Insights from direct sam-

- pling and the application of chemical box modeling, *J. Geophys. Res.*, *111*, D20206, doi:10.1029/2005JD006872.
- Salawitch, R. J., et al. (1993), Chemical loss of ozone in the Arctic polar vortex in the winter of 1991–1992, *Science*, *261*, 1146–1149.
- Schaefer, S. J., J. B. Kerr, M. M. Millán, V. J. Realmuto, A. J. Krueger, N. A. Krotkov, C. Seftor, and I. E. Sprod (1997), Geophysicists unite to validate volcanic SO₂ measurements, *Eos Trans. AGU*, *78*, 217.
- Schneider, D. J., W. I. Rose, L. R. Coke, G. J. S. Bluth, I. Sprod, and A. J. Krueger (1999), Early evolution of a stratospheric volcanic eruption cloud as observed with TOMS and AVHRR, *J. Geophys. Res.*, *104*, 4037–4050.
- Schoeberl, M. R., L. R. Lait, P. A. Newman, and J. E. Rosenfield (1992), The structure of the polar vortex, *J. Geophys. Res.*, *97*(D8), 7859–7882.
- Schoeberl, M. R., S. D. Doiron, L. R. Lait, P. A. Newman, and A. J. Krueger (1993), A simulation of the Cerro Hudson SO₂ cloud, *J. Geophys. Res.*, *98*(D2), 2949–2955.
- SEAN (1980), Hekla, *Smithsonian Scientific Event Alert Network*, 5(8).
- Seinfeld, J. H., and S. N. Pandis (2006), *Atmospheric Chemistry and Physics: From Air Pollution to Climate Change*, 2nd ed., John Wiley, Hoboken, N. J.
- Seftor, C. J., N. C. Hsu, J. R. Herman, P. K. Bhartia, O. Torres, W. I. Rose, D. J. Schneider, and N. Krotkov (1997), Detection of volcanic ash clouds from Nimbus 7/total ozone mapping spectrometer, *J. Geophys. Res.*, *102*(D14), 16,749–16,759.
- Serreze, M. C., and R. G. Barry (1988), Synoptic activity in the Arctic Basin, 1979–85, *J. Climate*, *1*(12), 1276–1295.
- Sharma, K., S. Blake, S. Self, and A. J. Krueger (2004), SO₂ emissions from basaltic eruptions, and the excess sulfur issue, *Geophys. Res. Lett.*, *31*, L13612, doi:10.1029/2004GL019688.
- Simkin, T., and L. Siebert (1994), *Volcanoes of the World*, 2nd ed., Geoscience Press, Tucson, Ariz.
- Smith, W. L., H. M. Woolf, C. M. Hayden, D. Wark, and L. M. McMillin (1979), The TIROS-N operational vertical sounder, *Bull. Am. Meteorol. Soc.*, *60*, 1177–1187.
- Soosalu, H., and P. Einarsson (2004), Seismic constraints on magma chambers at Hekla and Torfajökull volcanoes, Iceland, *Bull. Volcanol.*, *66*, 276–286.
- Soosalu, H., P. Einarsson, and B. S. Thorbjarnardóttir (2005), Seismic activity related to the 2000 eruption of the Hekla volcano, Iceland, *Bull. Volcanol.*, *68*, 21–36.
- Thorarinnsson, S. (1967), The eruptions of Hekla in historical times, in *The Eruption of Hekla 1947–48*, edited by T. Einarsson, G. Kjartansson, and S. Thorarinnsson, pp. 1–170, H. F. Leiftur, Reykjavik.
- Thorarinnsson, S., and G. E. Sigvaldason (1972), The Hekla eruption of 1970, *Bull. Volcanol.*, *36*, 269–288.
- Trenberth, K. E., and D. A. Paolino (1980), The Northern Hemisphere sea level pressure data set: Trends, errors, and discontinuities, *Mon. Weather Rev.*, *108*, 855–872. (Updated data available at <http://dss.ucar.edu/datasets/ds010.1/data/>)
- Tupper, A., S. Carn, J. Davey, Y. Kamada, R. Potts, F. Prata, and M. Tokuno (2004), An evaluation of volcanic cloud detection techniques during recent significant eruptions in the western “Ring of Fire”, *Remote Sens. Environ.*, *91*, 27–46.
- Wallace, P. (2005), Volatiles in subduction zone magmas: Concentrations and fluxes based on melt inclusion and volcanic gas data, *J. Volcanol. Geotherm. Res.*, *140*, 217–240.
- Watson, I. M., V. J. Realmuto, W. I. Rose, A. J. Prata, G. J. S. Bluth, Y. Gu, C. E. Bader, and T. Yu (2004), Thermal infrared remote sensing of volcanic emissions using the moderate resolution imaging spectroradiometer, *J. Volcanol. Geotherm. Res.*, *135*, 75–89.
- Yalcin, K., C. P. Wake, and M. Germani (2003), A 100-year record of North Pacific volcanism in an ice core from Eclipse Icefield, Yukon Territory, Canada, *J. Geophys. Res.*, *108*(D1), 4012, doi:10.1029/2002JD002449.
- Yalcin, K., C. P. Wake, K. J. Kreutz, M. S. Germani, and S. I. Whitlow (2007), Ice core paleovolcanic records from the St. Elias Mountains, Yukon, Canada, *J. Geophys. Res.*, *112*, D08102, doi:10.1029/2006JD007497.
- Yang, K., N. A. Krotkov, A. J. Krueger, S. A. Carn, P. K. Bhartia, and P. F. Levelt (2007), Retrieval of large volcanic SO₂ columns from the Aura Ozone Monitoring Instrument: Comparisons and limitations, *J. Geophys. Res.*, *112*, D24S43, doi:10.1029/2007JD008825.
- Zielinski, G. A., P. A. Mayewski, L. D. Meeker, S. Whitlow, M. S. Twickler, M. Morrison, D. A. Meese, A. J. Gow, and R. B. Alley (1994), Record of volcanism since 7000 B.C. from the GISP2 Greenland ice core and implications for the volcano-climate system, *Science*, *264*, 948–952.

S. A. Carn, Joint Center for Earth Systems Technology (JCET), University of Maryland Baltimore County (UMBC), 1000 Hilltop Circle, Baltimore, MD 21250, USA. (scarn@umbc.edu)

S. Karlsdóttir, Icelandic Meteorological Office, Bústaðarvegur 9, IS-150, Reykjavík, Iceland.

A. J. Prata, Atmosphere and Climate Department, Norwegian Institute for Air Research (NILU), Instituttveien 18, 2027 Kjeller, Norway.